



The following Communications have been judged by at least two referees to be “very important papers” and will be published online at www.angewandte.org soon:

H. Wu, H. Zhu, J. Zhuang, S. Yang, C. Liu, Y. C. Cao*
Water-Soluble Nanocrystals through Dual-Interaction Ligands

Y. V. Geletii, B. Botar,* P. Kögerler, D. A. Hillesheim, D. G. Musaev,
 C. L. Hill*

**An All-Inorganic, Stable, and Highly Active Tetraruthenium
 Homogeneous Catalyst for Water Oxidation**

Z. Liu, A. Kumbhar, D. Xu, J. Zhang, Z. Sun, J. Fang*
**Co-Reduction Colloidal Synthesis of III-V Nanocrystals: The Case
 of InP**

Y. H. Sehlleier, A. Verhoeven, M. Jansen*
**Observation of Direct Bonds Between Carbon and Nitrogen in
 Si–B–N–C Ceramic after Pyrolysis at 1400 °C**

H. Braunschweig,* C. J. Adams, T. Kupfer, I. Manners,
 R. Richardson, G. R. Whittell
**A Paramagnetic Polymer by Ring-Opening Polymerization of a
 Strained [1]Vanadoarenophane**

W. D. Pyrz, D. A. Blom, T. Vogt, D. J. Buttrey*
**Direct Imaging of the MoVTenbO M1 Phase Using an
 Aberration-Corrected High-Resolution Scanning Transmission
 Electron Microscope**

Obituary

Leslie E. Orgel (1927–2007)

Günter von Kiedrowski _____ 2338

Books

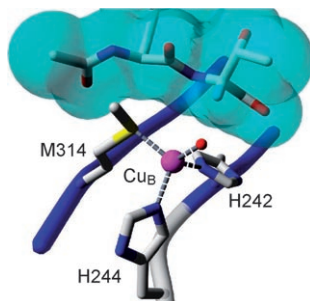
Nanotechnology in Biology and Medicine Tuan Vo-Dinh

reviewed by K. Kneipp _____ 2340

Computational Organic Chemistry Steven M. Bachrach

reviewed by B. Engels _____ 2340

Copper at work: The aliphatic ligand hydroxylation by a copper–oxygen center has been observed for the first time on a model system of the enzyme PHM (peptidylglycine- α -hydroxylating monooxygenase). This result is put in the context of the enzymatic mechanism, which presumably involves a high-valent copper oxo unit (violet-red) that hydroxylates the substrate (cyan).

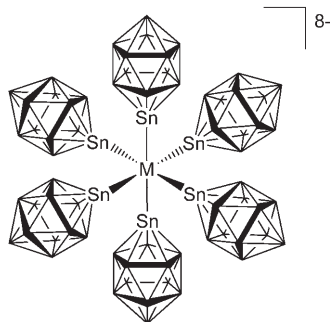


Highlights

Copper Monooxygenases

M. Rolff, F. Tuczek* _____ 2344–2347

How Do Copper Enzymes Hydroxylate Aliphatic Substrates? Recent Insights from the Chemistry of Model Systems



Encased in stannaborates: The synthesis of the homoleptic, octahedral M^{IV} complexes $[M(SnB_{11}H_{11})_6]^{8-}$ ($M = Ni, Pd, Pt$) has been reported. Spectroscopic data, together with the square-planar structure obtained for the corresponding tetrakis-ligated Ni^{II} complex $[Ni(SnB_{11}H_{11})_4]^{6-}$, provide ample evidence for the extremely strong σ -donor properties of the $[SnB_{11}H_{11}]^{2-}$ ligand.

Group 10 Complexes

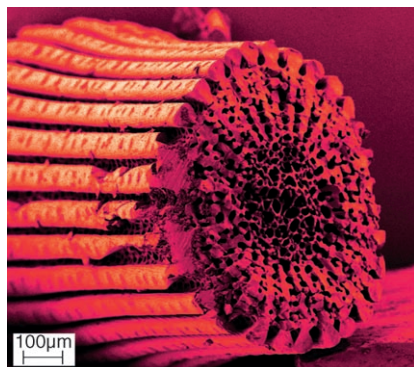
S. Aldridge* _____ 2348–2350

Exploitation of a Very Strongly σ -Donating Sn^{II} Ligand: Synthesis of a Homoleptic, Octahedral Ni^{IV} Complex

Crystal Growth

H. Cölfen* ————— 2351 – 2353

Single Crystals with Complex Form via Amorphous Precursors



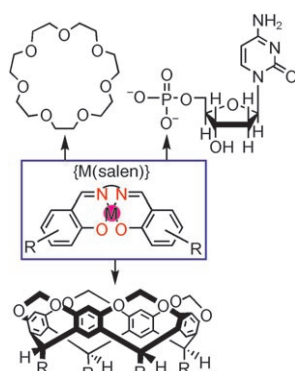
Nature is able to produce large single crystals with complex shape via amorphous precursor phases in the process of biomineralization (the picture shows an SEM image of a fracture surface of a sea urchin spicule). This strategy can be mimicked for the template synthesis of large single-crystalline materials with controllable complex shape.

Minireviews

Salen Frameworks

S. J. Wezenberg, A. W. Kleij* 2354 – 2364

Material Applications for Salen Frameworks



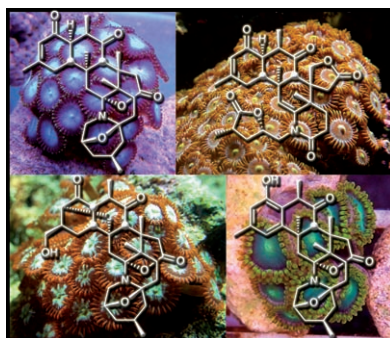
The salens are comin'! Salen synthons are becoming increasingly important for various chemical applications that go beyond their conventional use as versatile ligands in homogeneous catalysis. A recent increase in the use of these highly accessible building blocks has paved the way for the development of interesting hybrid materials with new catalytic, magnetic, and supramolecular properties.

Reviews

Marine Natural Products

D. C. Behenna, J. L. Stockdill,
B. M. Stoltz* ————— 2365 – 2386

The Biology and Chemistry of the Zoanthamine Alkaloids



More than meets the eye! Marine zoanthids have more to offer than stunning colors in home aquariums. They are the source of a host of fascinating natural products with great structural complexity and important biological activities. This Review chronicles the isolation and activity of zoanthamines, and describes the synthetic efforts toward this amazing class of natural products.

For the USA and Canada:

ANGEWANDTE CHEMIE International Edition (ISSN 1433-7851) is published weekly by Wiley-VCH, PO Box 191161, 69451 Weinheim, Germany. Air freight and mailing in the USA by Publications Expediting Inc., 200

Meacham Ave., Elmont, NY 11003. Periodicals postage paid at Jamaica, NY 11431. US POSTMASTER: send address changes to *Angewandte Chemie*, Wiley-VCH, 111 River Street, Hoboken, NJ 07030. Annual subscription price for institutions: US\$ 7225/6568 (valid for print and

electronic / print or electronic delivery); for individuals who are personal members of a national chemical society prices are available on request. Postage and handling charges included. All prices are subject to local VAT/sales tax.

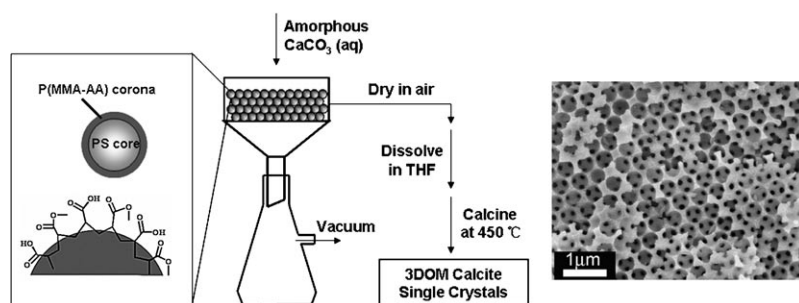
Communications

Colloidal Crystal Templating



C. Li, L. Qi* — 2388 – 2393

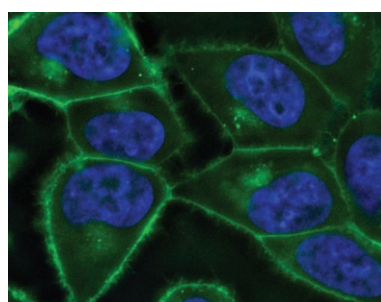
Bioinspired Fabrication of 3D Ordered Macroporous Single Crystals of Calcite from a Transient Amorphous Phase



Filling the gaps: Unique 3D ordered macroporous (3DOM) calcite single crystals with controlled orientation and well-defined nanopatterns are fabricated by introducing amorphous CaCO_3 into a

colloidal crystal template of polymer spheres (see picture). Such a bioinspired strategy suggests a route to functional single-crystalline materials and sheds light on biomineralization mechanisms.

Azide imaging: A fluorogenic phosphine based on a FRET-quenching mechanism allows for live-cell imaging of azido sugars by the Staudinger ligation. This design strategy can accommodate numerous fluorophores and complementary quenchers, enabling extension to multi-color imaging. In the image shown, the nuclei are blue while the cell surfaces and Golgi are green.



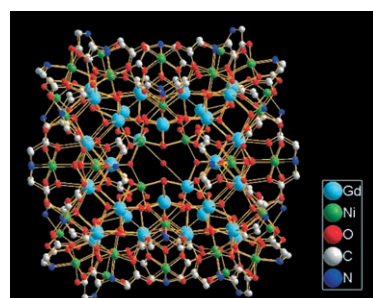
Live-Cell Imaging


M. J. Hangauer,
C. R. Bertozzi* — 2394 – 2397

A FRET-Based Fluorogenic Phosphine for Live-Cell Imaging with the Staudinger Ligation



A Russian doll: A heterometallic 108-metal cluster featuring an unprecedented four-shell, nesting doll-like structure (see picture) and overall antiferromagnetic coupling is reported.



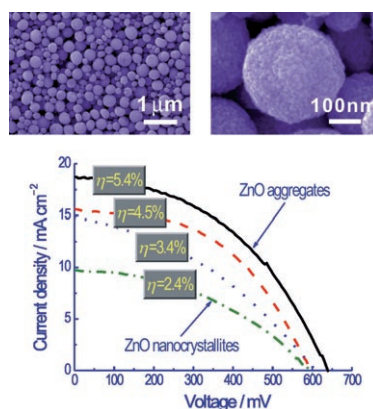
Heterometallic Clusters

X.-J. Kong, Y.-P. Ren, W.-X. Chen,
L.-S. Long,* Z. Zheng,* R.-B. Huang,
L.-S. Zheng — 2398 – 2401

A Four-Shell, Nesting Doll-like 3d-4f Cluster Containing 108 Metal Ions



Here comes the sun: A conversion efficiency as high as 5.4% has been achieved on dye-sensitized ZnO solar cells with photoelectrode films consisting of poly-disperse aggregates, compared to 2.4% for the films with only nanosized crystallites. The aggregation of nanocrystallites with a broad size distribution is effective in enhancing the light-harvesting efficiency by inducing light scattering within the photoelectrode films.



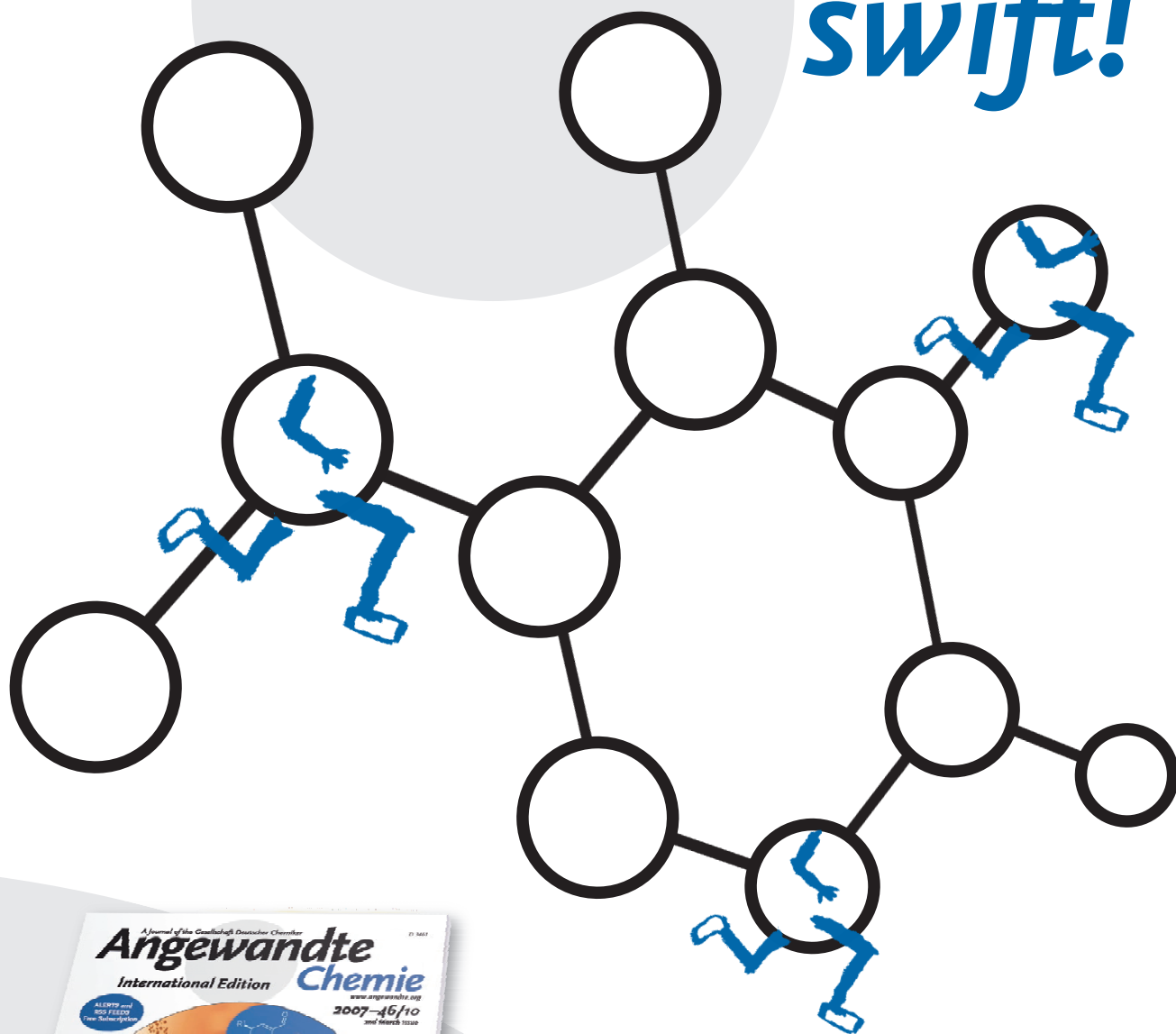
Dye-Sensitized Solar Cells


Q. F. Zhang, T. P. Chou, B. Russo,
S. A. Jenekhe, G. Z. Cao* — 2402 – 2406

Aggregation of ZnO Nanocrystallites for High Conversion Efficiency in Dye-Sensitized Solar Cells



Incredibly swift!



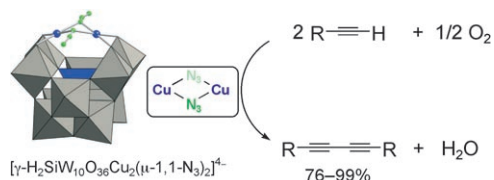
Manuscripts submitted to *Angewandte Chemie* can be published in a matter of days, and that's including meticulous peer review, copy-editing, and corrections. The peer-review process requires an average of just 13 days, and 30% of all Communications are brought to readers within two months after submission. The articles are not only published rapidly, they are also swiftly assimilated within the scientific community, as reflected by the extremely high Immediacy Index of *Angewandte Chemie* (2006: 2.106), meaning that each article in *Angewandte* is cited twice on average within the same year it was published.

service@wiley-vch.de
www.angewandte.org



GESELLSCHAFT
DEUTSCHER CHEMIKER





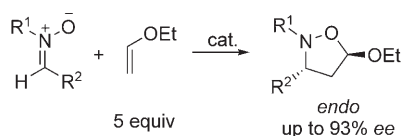
It goes on the dicopper core! A monomeric γ -Keggin silicotungstate with a dicopper core that is bridged by two μ -1,1-azido ligands catalyzes oxidative alkyne

homocoupling reactions whereby various kinds of aromatic and aliphatic alkynes are selectively converted into the corresponding diynes (see picture).

Homogeneous Catalysis

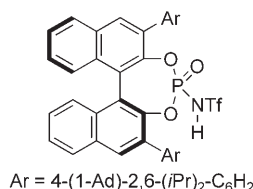
K. Kamata, S. Yamaguchi, M. Kotani, K. Yamaguchi, N. Mizuno* **2407–2410**

Efficient Oxidative Alkyne Homocoupling Catalyzed by a Monomeric Dicopper-Substituted Silicotungstate



Brønsted and Lewis face off: A new chiral *N*-triflyl phosphoramidate is used for asymmetric 1,3-dipolar cycloaddition of diaryl nitrones to ethyl vinyl ether to give the *endo* products in up to 93% *ee* (see

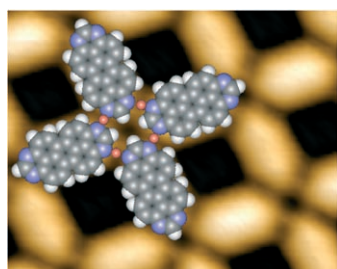
scheme; Tf = trifluoromethanesulfonyl; Ad = adamantyl). The structure of the chiral phosphoramidate was confirmed by X-ray crystallographic analysis.



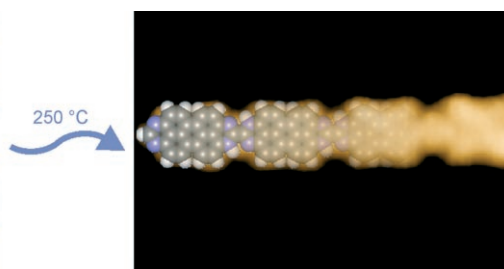
Asymmetric Synthesis

P. Jiao, D. Nakashima, H. Yamamoto* **2411–2413**

Enantioselective 1,3-Dipolar Cycloaddition of Nitrones with Ethyl Vinyl Ether: The Difference between Brønsted and Lewis Acid Catalysis



Isomerize and polymerize! Thermally induced tautomerization of the *N*-heteropolycyclic 1,3,8,10-tetraazaperopyrene to a Wanzlick-type carbene intermediate on a Cu(111) surface leads to covalently linked



polyaromatic chains, which can be mechanically manipulated. The pictures show the respective structures superimposed on the STM images.

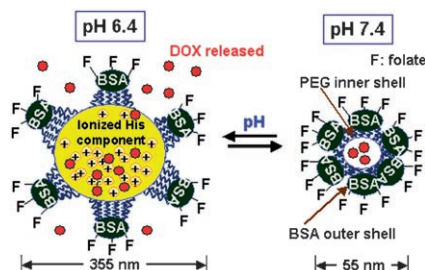
Surface Chemistry

M. Matena, T. Riehm, M. Stöhr,* T. A. Jung,* L. H. Gade* **2414–2417**

Transforming Surface Coordination Polymers into Covalent Surface Polymers: Linked Polycondensed Aromatics through Oligomerization of *N*-Heterocyclic Carbene Intermediates



Delivering the goods: A pH-sensitive nanogel consists of a hydrophobic copolymer core and two layers of hydrophilic shell (see picture). The core is loaded with a model anticancer drug, doxorubicin (DOX). The nanogel infects tumor cells in a receptor-dependent manner, kills the cells, and migrates to neighboring cells like a virus. BSA = bovine serum albumin, F = folate, PEG = polyethylene glycol.



Drug Delivery

E. S. Lee, D. Kim, Y. S. Youn, K. T. Oh, Y. H. Bae* **2418–2421**

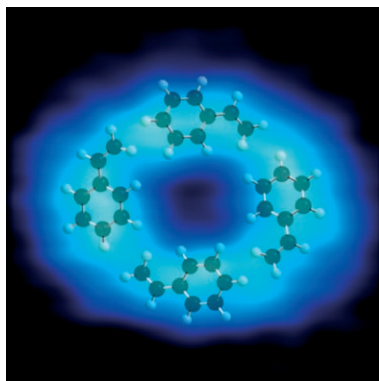
A Virus-Mimetic Nanogel Vehicle



Self-Assembly

O. P. H. Vaughan, A. Alavi, F. J. Williams,
R. M. Lambert* ————— 2422 – 2426

Dipole Amplification: A Principle for the Self-Assembly of Asymmetric Monomers on Metal Surfaces



Self-assembled nanostructures: Charge transfer from an adsorbed molecule to a metal surface induces an in-plane dipole moment that is strong enough to drive self-assembly. The STM image shows a styrene tetramer adsorbed on Ag(100). The dipole moment of styrene changes from 0.15 D in the gaseous state to 1.12 D in the adsorbed state. This substrate-induced dipole amplification is crucial to increasing the intermolecular interaction energy.



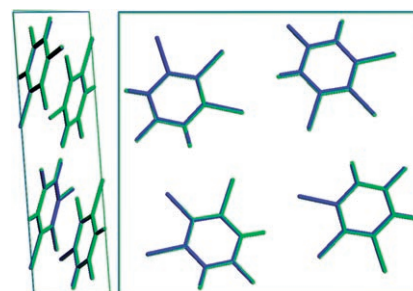
Crystal Structure Prediction

M. A. Neumann, F. J. J. Leusen,*
J. Kendrick ————— 2427 – 2430



A Major Advance in Crystal Structure Prediction

A crystal ball? A new method for crystal structure prediction combines a tailor-made force field with a density functional theory method incorporating a van der Waals correction for dispersive interactions. In a blind test, the method predicts the correct crystal structure for all four compounds, one of which is a cocrystal. The picture shows the predicted structure of one of the compounds in green and the experimental structure in blue.

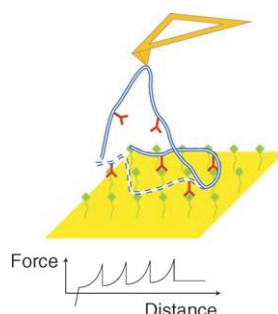


Single-Molecule Force Spectroscopy

F. Valle, G. Zuccheri, A. Bergia, L. Ayres,
A. E. Rowan, R. J. M. Nolte,
B. Samorì* ————— 2431 – 2434



A Polymeric Molecular “Handle” for Multiple AFM-Based Single-Molecule Force Measurements



Get a grip! The strategy of single-molecule mechanical unfolding of multimodular proteins is extended to the investigation of any chemical bond by an appropriately tailored, comblike polymer bearing multiple instances of any desired chemical interaction or bond to be studied along its linear chain. This approach is used to study the Ni-(His)_n-NTA complex (see picture: red, Ni-NTA; green, His tag; His = histidine; NTA = nitrilotriacetate).

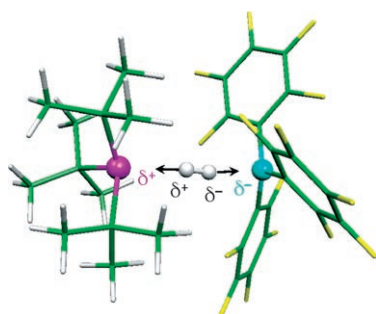


H₂ Activation

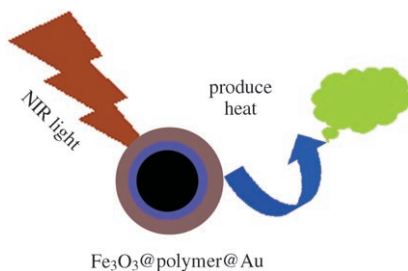
T. A. Rokob, A. Hamza, A. Stirling,
T. Soós,* I. Pápai* ————— 2435 – 2438



Turning Frustration into Bond Activation: A Theoretical Mechanistic Study on Heterolytic Hydrogen Splitting by Frustrated Lewis Pairs



Just before splitting: A mechanistic model has been proposed for H₂ activation by sterically demanding phosphine–borane Lewis pairs. There is theoretical evidence for noncovalent intermolecular association of donor–acceptor molecules to form a flexible but energetically strained complex, which provides preorganized active centers for heterolytic H–H bond cleavage (see picture).

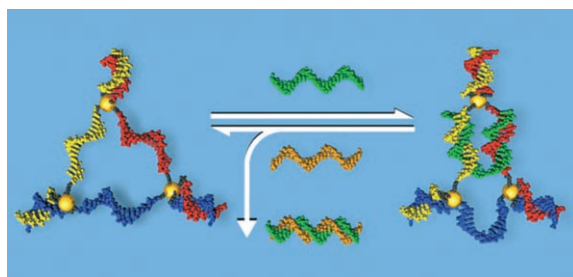


The best of both worlds: Multifunctional $\text{Fe}_3\text{O}_4@\text{polymer}@\text{Au}$ shell nanoparticles (see scheme; Fe_3O_4 is black, polymer is blue, gold shell is brown) display good dispersibility and stability in aqueous solution. Strong magnetization and good NIR absorption are preserved in the core-shell structures. These features should facilitate biomedical applications, combining the benefits of MRI diagnosis, magnetically targeted delivery, and photothermal ablation.

Magnetic Nanoparticles

L. Wang, J. Bai, Y. Li,
Y. Huang* ————— 2439–2442

Multifunctional Nanoparticles Displaying Magnetization and Near-IR Absorption



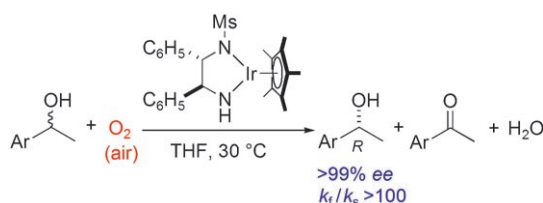
Templated metalation of DNA junctions allows incorporation of a range of transition metals into DNA assemblies. The resulting highly stable metal–DNA junctions can be assembled into dynamic multinuclear structures, with metal cen-

ters as their corners and DNA single strands as their sides. Ready and reversible structural switching of these assemblies with external agents (see picture) allows for control of geometry and metal–metal distances.

DNA Nanotechnology

H. Yang, H. F. Sleiman* — 2443–2446

Templated Synthesis of Highly Stable, Electroactive, and Dynamic Metal–DNA Branched Junctions



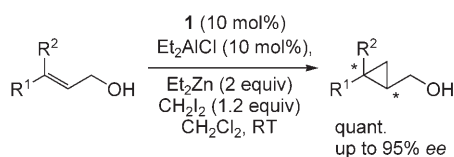
Up for air: The aerobic oxidative kinetic resolution of racemic secondary alcohols with chiral bifunctional Ir, Rh, and Ru catalysts proceeds smoothly under mild

conditions to provide chiral alcohols with up to 99% ee, and O_2 serves as an excellent hydrogen acceptor.

Aerobic Oxidation

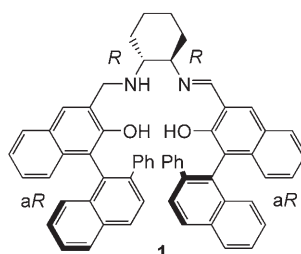
S. Arita, T. Koike, Y. Kayaki,
T. Ikariya* ————— 2447–2449

Aerobic Oxidative Kinetic Resolution of Racemic Secondary Alcohols with Chiral Bifunctional Amido Complexes



Three angles: A highly enantioselective Simmons–Smith reaction of *trans*-disubstituted allylic alcohols was achieved by

using a catalytic amount of an Al(salalen) complex at room temperature (see scheme).



Asymmetric Catalysis

H. Shitama, T. Katsuki* — 2450–2453

Asymmetric Simmons–Smith Reaction of Allylic Alcohols with Al Lewis Acid/ N Lewis Base Bifunctional Al(salalen) Catalyst

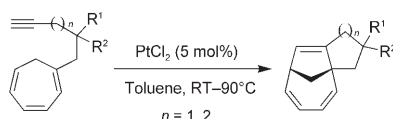


Cyclization

A. Tenaglia,* S. Gaillard — 2454–2457



PtCl₂-Catalyzed [6+2] Cycloaddition of Alkynes Tethered to Cycloheptatriene



Summing up the situation: Eight-membered rings can be synthesized in an intramolecular formal [6+2] cycloaddition of alkynylcycloheptatrienes catalyzed by PtCl₂ (see scheme). The use of heteroatom-tethered substrates provide complex heterocyclic compounds, while the use of a higher temperature leads to an unusual formal [6+1] cycloaddition.

Multicomponent Reactions

J. Jiang, J. Yu, X.-X. Sun, Q.-Q. Rao, L.-Z. Gong* — 2458–2462



Organocatalytic Asymmetric Three-Component Cyclization of Cinnamaldehydes and Primary Amines with 1,3-Dicarbonyl Compounds: Straightforward Access to Enantiomerically Enriched Dihydropyridines



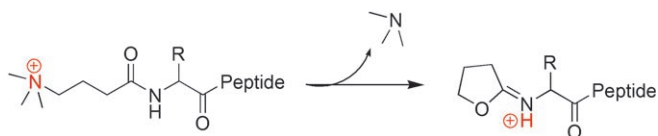
All in together: The title reaction takes place under mild conditions in the presence of a chiral phosphonic acid catalyst to provide 4-aryl substituted 1,4-dihydropyridines with up to 98 % *ee* (see scheme). The products are useful substrates for the

asymmetric synthesis of tetrahydropyridines and multifunctional piperidines, which are common substructures of natural products and pharmaceuticals. R¹ = aryl; R², R³ = alkyl.

Peptide Mass Spectrometry

Y. He, J. P. Reilly* — 2463–2465

Does a Charge Tag Really Provide a Fixed Charge?



Tag along for the ride: A peptide derivatized with a quaternary ammonium charge tag is collisionally dissociated. Observation of both N- and C-terminal fragment

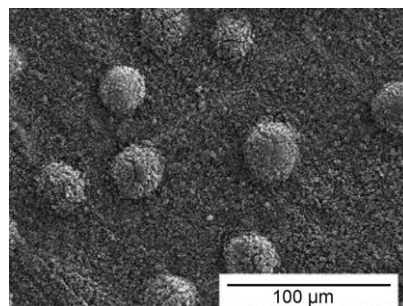
ions demonstrates that a mobilized proton is produced during the dissociation process (see scheme).

Corrosion Protection

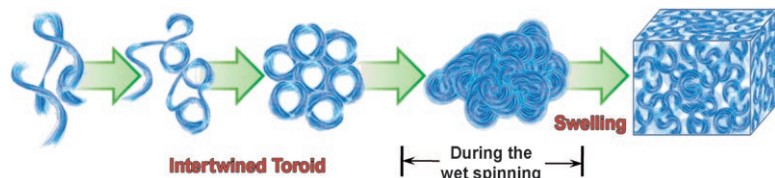
F. Z. Zhang, L. L. Zhao, H. Y. Chen, S. L. Xu, D. G. Evans, X. Duan* — 2466–2469



Corrosion Resistance of Superhydrophobic Layered Double Hydroxide Films on Aluminum



Laurate-intercalated films of ZnAl layered double hydroxide (ZnAl-LDH-laurate) were fabricated by anion exchange of laurate with ZnAl-LDH-NO₃[−] films on a porous anodic alumina/aluminum (PAO/Al) substrate. The presence of both microscale and nanoscale hierarchical structures (see SEM image) makes the film superhydrophobic, and thus it has much better corrosion resistance than anodic PAO film alone or ZnAl-LDH-NO₃[−] films.



Spinning strands: A hydrogel fiber made entirely of DNA without any covalent cross-links, composed of intertwined toroid entanglements of flexible DNA strands (see scheme), was prepared by a one-step wet-spinning method with a

hydrophilic ionic liquid as the condensing agent and coagulation solvent. The internal structure of the fiber was a disordered arrangement of strands with a B-DNA form. The fiber was also stable in various aqueous solutions.

DNA Structures

C. K. Lee, S. R. Shin, S. H. Lee, J.-H. Jeon, I. So, T. M. Kang, S. I. Kim, J. Y. Mun, S.-S. Han, G. M. Spinks, G. G. Wallace, S. J. Kim* **2470–2474**

DNA Hydrogel Fiber with Self-Entanglement Prepared by Using an Ionic Liquid



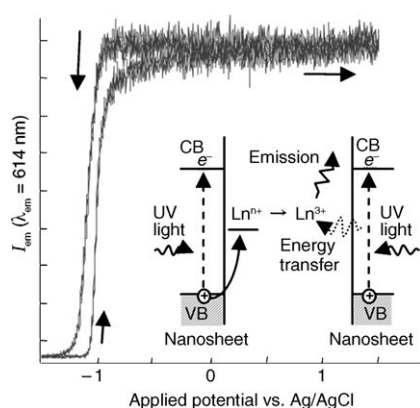
A good neighbor is better than a far-away friend: A tethering strategy is used to self-select groups that assist in the cleavage of a neighboring carboxylic ester moiety (see

picture, TSA = transition-state analogue). A correlation is observed between the amplification at thermodynamic equilibrium and the catalytic efficiency.

Dynamic Selection

G. Gasparini, L. J. Prins,* P. Scrimin* **2475–2479**

Exploiting Neighboring-Group Interactions for the Self-Selection of a Catalytic Unit

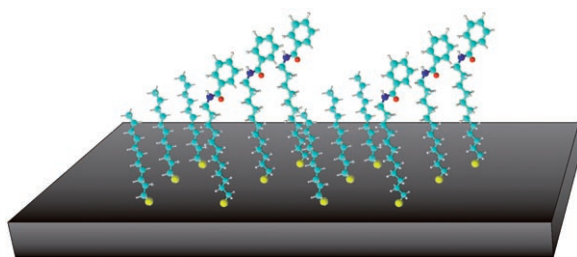


Getting turned on: A photoelectrochemical reaction has been used to control the photoluminescence of self-assembled nanosheet films intercalated with Ln^{3+} ions. Emission (em) occurs under anodic bias (mechanism shown) and not under cathodic bias because of the oxidation and reduction of $\text{Ln}^{3+}/\text{Ln}^{n+}$ by holes and electrons by UV light, respectively (see picture, VB = valence band, CB = conduction band), which allows control of the emission on/off response.

Luminescence

S. Ida,* C. Ogata, D. Shiga, K. Izawa, K. Ikeue, Y. Matsumoto **2480–2483**

Dynamic Control of Photoluminescence for Self-assembled Nanosheet Films Intercalated with Lanthanide Ions by Using a Photoelectrochemical Reaction



Controlled confinement: A supramolecular approach for the design of multi-component self-assembled monolayers on Au(111) is employed to obtain subnanometer-resolved patterns on the solid

substrate (see picture). The formation of crystalline bicomponent domains is discussed in view of their potential applications in the development of new electronic devices.

Scanning Probe Microscopy

G. Pace, A. Petitjean, M.-N. Lalloz-Vogel, J. Harrowfield, J.-M. Lehn,* P. Samori* **2484–2488**

Subnanometer-Resolved Patterning of Bicomponent Self-Assembled Monolayers on Au(111)

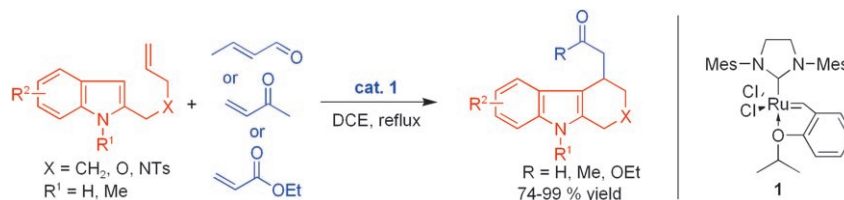


Tandem Reactions

J.-R. Chen, C.-F. Li, X. L. An, J.-J. Zhang,
X.-Y. Zhu, W.-J. Xiao* — 2489–2492



Ru-Catalyzed Tandem Cross-Metathesis/
Intramolecular-Hydroarylation Sequence



Sometimes it only takes one to tango: A novel ruthenium-catalyzed tandem cross-metathesis/intramolecular-hydroarylation reaction of alkenyl indoles has been developed which relies on a single catalyst for the tandem sequence and provides an

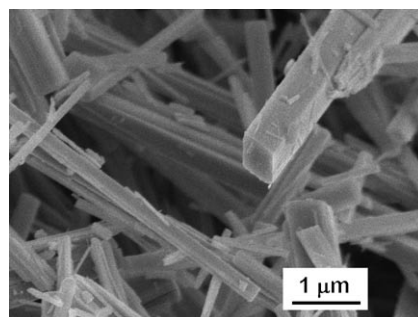
efficient synthesis of fused polycyclic indole compounds with good to excellent overall yields (see scheme; Ts = 4-toluenesulfonyl, DCE = 1,2-dichloroethane, Mes = 2,4,6-Me₃C₆H₂).

Molecular Sieves

M. Sadakane,* K. Kodato, T. Kuranishi,
Y. Nodasaka, K. Sugawara, N. Sakaguchi,
T. Nagai, Y. Matsui,
W. Ueda* — 2493–2496



Molybdenum–Vanadium-Based
Molecular Sieves with Microchannels of
Seven-Membered Rings of Corner-Sharing
Metal Oxide Octahedra



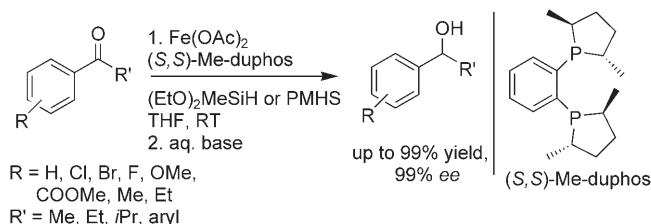
Octahedral molecular sieves: Crystalline orthorhombic Mo₃VO_x (see SEM image), which was prepared by hydrothermal synthesis, contains microchannels made up of seven-membered rings of corner-sharing {MO₆} octahedra. Small molecules such as methane, ethane, N₂, Ar, CO₂ can enter the microchannels of this compound, which exhibits the type I adsorption behavior typical of microporous materials.

Iron Catalysis

N. S. Shaikh, S. Enthaler, K. Junge,
M. Beller* — 2497–2501



Iron-Catalyzed Enantioselective
Hydrosilylation of Ketones



Reductions under iron rule: Enantioselective hydrosilylation of prochiral ketones with inexpensive and environmentally benign iron catalysts proceed smoothly in the presence of (*S,S*)-Me-duphos (see scheme; (*S,S*)-Me-duphos = 1,2-(bis-

[(2*S*,5*S*)]-2,5-dimethylphospholano)benzene). A broad range of aryl ketones is converted into the corresponding secondary alcohols in up to 99% enantioselectivity and quantitative yields.

Olefin Oxygenation

M. P. del Río, M. A. Ciriano,
C. Tejel* — 2502–2505



From Olefins to Ketones via a
2-Rhodaioxetane Complex



Quantitative oxygenation of 1,5-cyclooctadiene to 4-cyclooctenone with molecular oxygen by a rhodium complex proceeds via a 2-rhoda(III)oxetane intermediate

(see scheme), which undergoes a facile β-elimination reaction to give the unsaturated ketone selectively instead of the epoxide.

